The Deformable-Channel Model—A New Approach to High-Frequency MESFET Modeling

FRANK J. CROWNE, ABDOLLAH ESKANDARIAN, H. BRIAN SEQUEIRA, AND RAJENDRA JAKHETE

Abstract—**High-frequency small-signal circuit parameters are evaluated for a saturated-channel MESFET by including transit-time effects in a rigorous way through a study of induced shape changes in the saturated-channel region. Results agree well with empirical equivalent-circuit parameters for a physical MESFET.**

I. Introduction

THE INHERENT material properties of GaAs, that is, its high electron mobility (~ 5000 cm^2/V-s) and high saturation velocity ($\simeq 1.2\times10^7$ cm/s) [1], along with the availability of semi-insulating GaAs substrates with resistivities on the order of 10^6–10^8 $\Omega\cdot$cm, have made GaAs MESFET's the active devices of choice in designing monolithic microwave and millimeter-wave integrated circuits. The major advantage of the monolithic approach [2] over the hybrid approach is well known: various parasitic impedances derived from the components of the hybrid structure (i.e., bond wires, bends, and interconnections) are avoided. However, the major disadvantage of the monolithic approach is equally well known: once built, an integrated circuit cannot be adjusted by the trial-and-error methods used by designers of hybrid circuits. It is therefore imperative that an accurate device model be employed to characterize the MESFET's used in a given monolithic circuit. Furthermore, because of the complexity of the circuit problem itself, such a model should be analytic rather than numerical in order to facilitate computer simulation. Unfortunately, the physics of MESFET operation are so complex that no single analytic model exists at this time that can accurately describe MESFET performance at all frequencies and terminal voltages.

The most successful dc MESFET model to date is the two-region model of Grebene and Ghandhi [3], which crudely accounts for velocity saturation by assuming the piecewise-linear velocity-field curve shown in Fig. 1. This model divides the MESFET channel into two regions. In the region adjacent to the source, the gradual-channel approximation is assumed to be valid. The rest of the channel up to the drain consists of a thin change-neutral sheet of undepleted free carriers moving at the saturated velocity of the MESFET material. (We refer to this portion of the channel as "saturated.") The width of this sheet is assumed to be constant for a given drain current, whereas its length (i.e., the length of the second region) is a function of the terminal voltages. A strongly two-dimensional field distribution is assumed to exist in the second region, originating from charges beyond the drain end of the gate. This field ensures that the carriers move at the saturation velocity and that all of the voltage drop across the saturated part of the channel is accounted for. This model gives an adequate set of I–V curves for a MESFET under dc bias conditions.

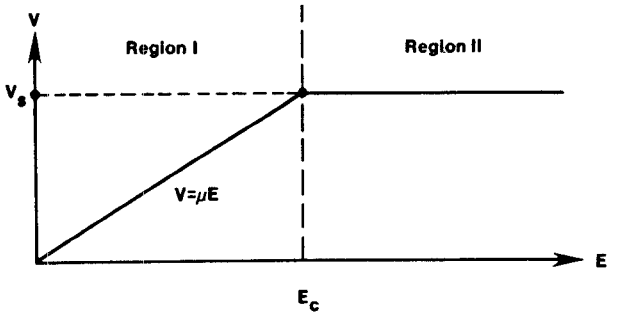

Fig. 1. Velocity-field relation for the two-region model

Pucel *et al.* [4] derived the small-signal parameters for this model using a quasi-dc approach; the equivalent circuit was subsequently extended to higher frequencies by Vendelin and Omori [5], who arrived at the equivalent circuit shown in Fig. 2(a). In this figure, g_m denotes the dc transconductance, while r_{ds} and C_{ds} are the drain-to-source resistance and capacitance. C_{gs} is the gate-to-source capacitance and C_{dg} the drain-to-gate capacitance; these capacitances are determined by a procedure, described by Pucel *et al.*, in which part of the gate charge is assumed to be controlled by the gate-to-source voltage, and the rest by the drain-to-gate voltage. Convincing oneself that such an approach must always lead to the same equivalent circuit topology, given the assumption that no dc current flows from gate to source, is not hard. The quasi-dc approach can be naively justified by noting that for a free carrier

Manuscript received March 17, 1987; revised August 17, 1987.
The authors are with Martin Marietta Laboratories, Baltimore, MD 21227-3898
IEEE Log Number 8717498.

0018-9480/87/1200-1199$01.00 ©1987 IEEE

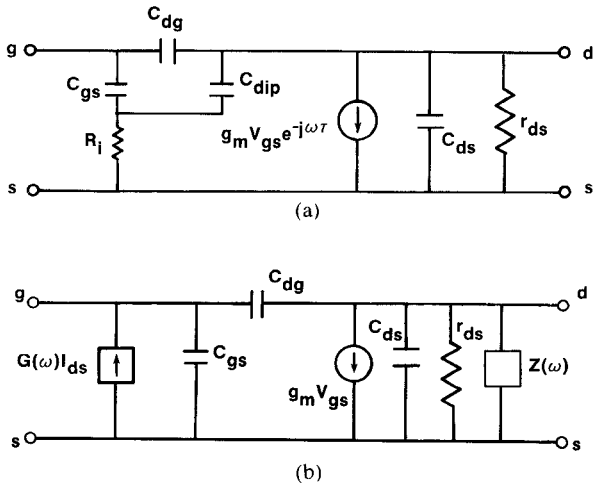

Fig. 2. (a) High-frequency MESFET equivalent circuit; the elements C_{dip}, R_i, and τ are all empirical parameters. (b) Deformable-channel equivalent circuit.

density of 10^{17} cm^{-3} and a mobility of 10^3 cm^2 (V·s)$^{-1}$, the dielectric relaxation time for the undepleted channel regions is $\tau = \epsilon/\sigma \sim 10^{-13}$ s. This suggests that the free charges can redistribute themselves almost instantly when the terminal voltages change, moving in such a way as to restore the dc relations between current and voltage.

Because of their short gate lengths, high-frequency MESFET's operate under bias conditions that ensure that almost all the channel is "saturated" [6]. This circumstance suggests that transit-time effects, which by definition violate the quasi-dc assumption, will dominate the device ac response, and that therefore the quasi-dc picture should be reexamined. Indeed, the quantities R_i, C_{dip}, and τ (shown in Fig. 2(a)), which are related to transit-time effects, are all obtained by curve fitting and cannot usually be obtained from any model [7].

We present here a new model for the ac response of a MESFET under these special conditions. Our model includes transit-time effects from the outset and allows us to go beyond the quasi-dc approximation in describing the ac behavior of the MESFET. The basic new physics of the device operation are discussed in Section II; a thorough mathematical treatment is presented in Section III; and modeling results and experimental results are compared in Section IV.

II. The Deformable Channel

The argument presented in Section I as a justification for the quasi-dc approach cannot be sustained for the saturated channel region. This is because the dielectric relaxation time for a charge inhomogeneity in a nonlinear material (i.e., a material in which the drift velocity v_D of a carrier due to an applied electric field E_0 is not simply equal to μE_0 where μ is the low-field mobility) is determined by the *differential* mobility

$$\tilde{\mu} = \left.\frac{dv_D}{dE}\right|_{E=E_0} \tag{1}$$

which is very small (in fact, negative) in the saturated-channel region for GaAs. The result of this is well known in the theory of IMPATT's: [8] charge inhomogeneities do not decay at all, but rather propagate across the drift region of the IMPATT. This effect is, of course, well understood by MESFET modelers, but its consequences for a MESFET are difficult to quantify. In the IMPATT, charge inhomogeneities propagate in the form of *longitudinal* waves through the drift region of the device, with no transverse current flow; this is a consequence of the device geometry. In the MESFET channel, where the geometry is that of a thin sheet, the transverse currents cannot be ignored. Indeed, under high-field conditions the mobility is a highly anisotropic quantity: transverse to the channel it should assume its low-field value. From these facts we draw the following conclusion: charge inhomogeneities that appear in the saturated channel relax quickly, changing the channel *shape* locally. That is, a region of the channel for which the free charge is greater than the doping density N_D quickly becomes a region in which the channel width is larger than normal. This comes about because excess charge is free to flow into the depletion region on a time scale $\sim 10^{-13}$ s and restore local charge neutrality. Likewise, when the free charge is less than N_D, the channel contracts. These shape variations are assumed to propagate down the channel just as compressional waves do in the drift region of an IMPATT and, as we will show in Section III, can significantly affect the ac impedances of the device.

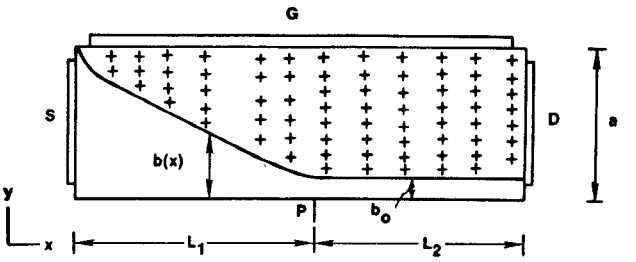

Fig. 3. Schematic of a MESFET for the two-region model.

III. Mathematical Description

A. Preliminaries

Let us assume that the device geometry is the same as that shown in Fig. 3: an epitaxial layer of length L and width a, with a donor doping density of N_D. The width of the saturated channel under dc conditions is denoted by b_0 and is determined within the two-region model by the gate and source–drain voltages. Let $\delta I_D(x,t)$ be the spatially dependent total ac current flowing in the channel and passing through a plane located at the point x. Because of velocity saturation, the continuity equation then reads

$$\frac{\partial}{\partial t}\delta I_D = -v_s \frac{\partial}{\partial x}\delta I_D \tag{2}$$

which is the same equation as the one used in IMPATT theory; v_s is the saturation velocity. Let $x = L_1$ be the end of the gradual channel. Then

$$\delta I_D(L_1, t) = \tilde{\delta} I_D e^{+j\omega t} \tag{3}$$

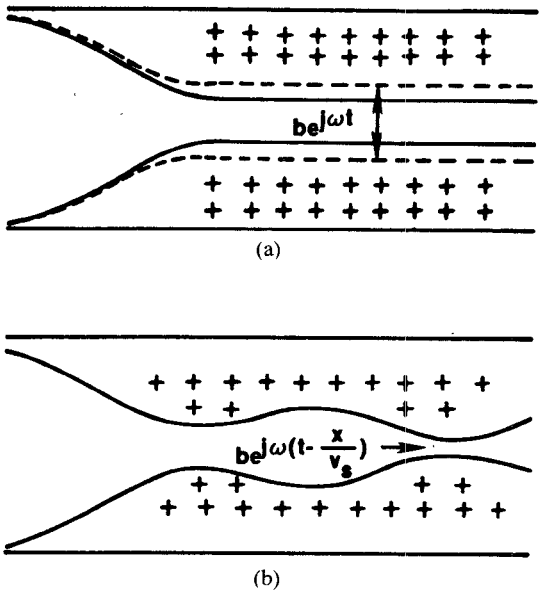

Fig. 4. Motion of a saturated MESFET channel. (a) "Breathing," which accompanies an ac drain current. (b) Propagation of a shape distortion in the transit-time regime.

where $\tilde{\delta}I_D$ is the source terminal ac current. Equation (3) implies that the gradual-channel part of the MESFET responds instantaneously to a change in current at the terminals. Then (3) and (2) imply that

$$\delta I_D(x,\ t) = \tilde{\delta}I_D e^{j\omega[t-\frac{1}{v_s}(x-L_1)]}, \qquad x \geqslant L_1$$

for the current at each point in the channel. Now, let us assume that the only way δI_D can vary is through a change in the channel height δb; this is again consistent with the assumption of instantaneous local charge neutrality. Then

$$\delta I_D(x,t) = N_D e v_s z \delta b(x,t)$$

where z is the gate width. This implies that

$$\delta b = \frac{1}{N_D e v_s z}\delta I_D = \left[\hat{\delta}b_{\mathrm{LF}} + \hat{\delta}b(x)_{\mathrm{HF}}\right]e^{j\omega t}$$

where

$$\hat{\delta}b_{\mathrm{LF}} = \frac{\tilde{\delta}I_D}{N_D e v_s z}$$

and

$$\hat{\delta}b(x)_{\mathrm{HF}} = \hat{\delta}b_{\mathrm{LF}}\left[e^{-j\frac{\omega}{v_s}(x-L_1)}-1\right]. \tag{4}$$

We have divided the channel width variation into two parts: a low-frequency "breathing" part $\hat{\delta}b_{\mathrm{LF}}$, which corresponds to the channel expanding and contracting *as a whole*, and a part $\hat{\delta}b_{\mathrm{HF}}$, which contains the propagation (i.e., transit-time) effects. These contributions are illustrated in Fig. 4, where we have adopted the symmetric JFET geometry used by Grebene and Ghandhi (i.e. two identical devices joined together along $y = 0$). Note that if $\omega \to 0$ or $v_s \to \infty$, our $\hat{\delta}b_{\mathrm{HF}}$ term vanishes; it is thus an intrinsically high-frequency quantity. If we proceed to calculate the effect of $\hat{\delta}b_{\mathrm{LF}}$ alone on the terminal characteristics, and

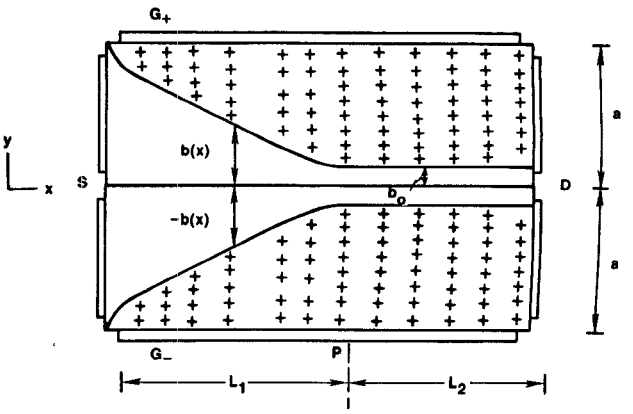

Fig. 5. Symmetric MESFET geometry.

ignore $\hat{\delta}b_{\mathrm{HF}}$ entirely, we recover the small-signal results of Pucel *et al.*, which are in fact based on this breathing motion of the channel.

The two-dimensional Poisson equation for the potential in the saturated-channel region now reads

$$\left(\frac{\partial^2}{\partial x^2}+\frac{\partial^2}{\partial y^2}\right)V(x,y;t) = \frac{e}{\epsilon_r\epsilon_0}\left[n(x,y;t)-N_D\right]. \tag{5}$$

The symmetric geometry of Grebene and Ghandhi as shown in Fig. 5 simplifies the analysis greatly. Then

$$n(x,y;t) = N_D\left[\theta(y+b(x,t))-\theta(y-b(x,t))\right]$$

where we introduce the usual step function

$$\theta(X) = \begin{cases}1, & X>0\\ 0, & X<0\end{cases}$$

to describe the free-carrier density. Let us write

$$n(x,y;t) = n_0(x,y)+\hat{\delta}n(x,y)e^{j\omega t}$$
$$b(x,t) = b_0+\hat{\delta}b(x)e^{j\omega t}.$$

Assuming that $\hat{\delta}b$ is small,

$$\theta(y\pm b(x,t)) = \theta\left(y\pm b_0\pm\hat{\delta}b\right)$$
$$\cong \theta(y\pm B_0)\pm\hat{\delta}b(x)\delta(y\pm b_0)$$

where $\delta(x)$ is the Dirac δ-function. If now

$$n_0(x,y) = N_D\left[\theta(y+b_0)-\theta(y-b_0)\right]$$

and

$$\hat{\delta}n(x,y) = N_D\left[\delta(y+b_0)+\delta(y-b_0)\right]\hat{\delta}b(x)$$

equating zero- and first-order terms in (5) gives

$$\left(\frac{\partial^2}{\partial x^2}+\frac{\partial^2}{\partial y^2}\right)V_0(x,y) = \frac{e}{\epsilon_r\epsilon_0}\left[n_0(x,y)-N_D\right] \tag{6}$$

and

$$\left(\frac{\partial^2}{\partial x^2}+\frac{\partial^2}{\partial y^2}\right)\hat{\delta}V(x,y) = \frac{N_D e}{\epsilon_r\epsilon_0}\left[\delta(y+b_0)+\delta(y-b_0)\right]\hat{\delta}b(x). \tag{7}$$

Grebene and Ghandhi solve (6); (7) gives the high-frequency correction to the potential in the saturated chan-

nel region. Actually, we can now write

$$\hat{\delta V}(x, y) = \hat{V}_{\mathrm{LF}}(x, y) + \hat{V}_{\mathrm{HF}}(x, y)$$

where the subscripts refer to the corresponding parts of $\hat{\delta b}$. The potential $\hat{V}_{\mathrm{LF}}$ now is precisely the small-signal "breathing" correction to the saturated channel potential; by solving for it we recover the expressions found in Pucel *et al.*, while

$$\left(\frac{\partial^2}{\partial x^2} + \frac{\partial^2}{\partial y^2}\right)\hat{V}_{\mathrm{HF}}(x, y) = \frac{N_D e}{\epsilon_r \epsilon_0}\left[\delta(y + b_0) + \delta(y - b_0)\right]\hat{\delta b}_{\mathrm{HF}}(x) \quad (8)$$

is the (two-dimensional) correction at high frequencies, and $\hat{\delta b}_{\mathrm{HF}}$ is half the value given in (4) due to the two contributions to δI_D.

B. Solution to the High-Frequency Equation

In order to solve (8), we must assume some boundary conditions for the 2-D region. An immediate condition is that the perturbation of the potential vanishes under the metal gate (i.e., at $y = \pm a$):

$$\hat{V}_{\mathrm{HF}}(x, \pm a) = 0.$$

We can ensure this by writing

$$\hat{V}_{\mathrm{HF}}(x, y) = \sum_{n=0}^{\infty} V_n(x)\cos\Gamma_n y$$

where

$$\Gamma_n = \left(n + \frac{1}{2}\right)\frac{\pi}{a}.$$

Note that the symmetric geometry results in only cosine terms. Now, we also can write

$$\delta(y + b_0) + \delta(y - b_0) = \sum_{n=0}^{\infty} J_n \cos\Gamma_n y$$

where

$$J_n = \frac{2}{a}\cos\Gamma_n b_0.$$

This decouples the Fourier components of the solution to (8), each of which now satisfies an equation

$$\left(\frac{\partial^2}{\partial x^2} - \Gamma_n^2\right)V_n(x) = \frac{N_D e}{\epsilon_r \epsilon_0} J_n \hat{\delta b}_{\mathrm{HF}}(x) = QJ_n\left[e^{-j\frac{\omega}{v_s}(x - L_1)} - 1\right] \quad (9)$$

where

$$Q = \frac{\tilde{\delta I}_D}{2z\epsilon_r\epsilon_0 v_s}.$$

and the factor of 2 comes from the symmetric device geometry. At this point, we face the same problem as Grebene and Ghandhi: what boundary condition do we assume at the ends of the channel? If we assume that the perturbation vanishes at the $x = L_1$ plane, we will at least be guaranteed continuity of the potential across the plane (i.e., a match with the gradual channel solution). However, it is *not* correct to also specify the normal derivative of $\hat{V}_{\mathrm{HF}}$ on this plane, as Grebene and Ghandhi (implicitly) did; the Poisson equation requires a boundary condition on the plane $x = L$ (i.e., the end of the channel), either Dirichlet or Neumann, to give a unique, stable solution [9]. We will assume that the normal field falls sharply at this point, since the channel will begin to "open up" beyond it and the relaxation time will return to its bulk value, thereby "shorting out" the high-frequency perturbation. Then

$$\left.\frac{\partial}{\partial x}\hat{V}_{\mathrm{HF}}(x, y)\right|_{x = L} = 0. \quad (10)$$

Now, any solution to (9) is of the form

$$V_n(x) = A_n e^{\Gamma_n(x - L_1)} + B_n e^{-\Gamma_n(x - L_1)} + C_n + D_n e^{-j\frac{\omega}{v_s}(x - L_1)}$$

where A_n, B_n, C_n, and D_n are constants. It is easy to show that

$$C_n = \frac{+QJ_n}{\Gamma_n^2}$$

$$D_n = \frac{-QJ_n}{k_s^2 + \Gamma_n^2}$$

where $k_s = \omega/v_s$. Using

$$\hat{V}_{\mathrm{HF}}(L_1, y) = 0$$

and condition (10) gives

$$A_n = \frac{-QJ_n k_s}{2\Gamma_n^2 \cosh\Gamma_n L_2} \cdot \frac{k_s e^{-\Gamma_n L_2} + i\Gamma_n e^{-jk_s L_2}}{k_s^2 + \Gamma_n^2}$$

$$B_n = \frac{-QJ_n k_s}{2\Gamma_n^2 \cosh\Gamma_n L_2} \cdot \frac{k_s e^{\Gamma_n L_2} - i\Gamma_n e^{-jk_s L_2}}{k_s^2 + \Gamma_n^2}$$

and $L_2 = L - L_1$ is the length of the saturated channel.

C. Calculation of Terminal Parameters

Because of the change in potential in the saturated channel, there are two new contributions to the terminal parameters: an additional voltage drop down the channel and an additional charge induced on the gates. The voltage drop is simply

$$\begin{aligned}\Delta\hat{V}_{\mathrm{HF}} &= \hat{V}_{\mathrm{HF}}(L, 0) \\ &= \sum_{n=0}^{\infty} V_n(L) \\ &= \sum_{n=0}^{\infty} A_n e^{\Gamma_n L_2} + B_n e^{-\Gamma_n L_2} + C_n + D_n e^{-jk_s L_2}.\end{aligned}$$

Note that the constants A_n, B_n, C_n, and D_n are all proportional to Q (i.e., to $\tilde{\delta I}_D$). Hence,

$$\Delta\hat{V}_{\mathrm{HF}} = Z(\omega)\hat{\delta I}_D.$$

Since this voltage adds directly to V_D, the impedance $Z(\omega)$ should add directly to the r_{ds} calculated by Pucel *et al.*

$Z(\omega)$ is a pure transit-time impedance, i.e., it reflects the fact that charge is stored in the saturated channel due to the finite travel time across the device.

To find the charge induced on the (upper and lower) gates, we follow Grebene and Ghandhi:

$$\delta Q_{\mathrm{HF}} = +2\epsilon_r\epsilon_0 z\int_{L_1}^{L_2} -\frac{\partial}{\partial y}\hat{V}_{\mathrm{HF}}(x,y)\bigg|_{y=a} dx$$

$$= -2\epsilon_r\epsilon_0 z\sum_{n=0}^{\infty}\Big[(-1)^n A_n(e^{\Gamma_n L_2}-1)+B_n(1-e^{-\Gamma_n L_2}) + C_n\Gamma_n L_2 + D_n\frac{j\Gamma_n}{k_2}(e^{-jk_s L_2}-1)\Big].$$

If we now write the ac gate current as

$$\tilde{\delta I}_G = j\omega\delta\tilde{Q}_{\mathrm{HF}}$$

then

$$\tilde{\delta I}_G = -G(\omega)\tilde{\delta I}_D$$

where $G(\omega)$ defines a current-controlled current source that depends on frequency.

Let us derive the Y matrix including these new small-signal elements. From the equivalent circuit shown in Fig. 2(b), we have for the intrinsic FET alone ($C_{dg}=C_{ds}=0$):

$$\delta I_{\mathrm{in}} = j\omega C_{gs} - G(\omega)\delta I_D$$
$$= j\omega C_{gs} + G(\omega)\delta I_{\mathrm{out}}$$

and

$$\delta I_{\mathrm{out}} = g_m\delta V_g + r_{ds}^{-1}(\delta V_{ds} + Z(\omega)\delta I_D)$$
$$= g_m\delta V_g + r_{ds}^{-1}\delta V_{ds} - r_{ds}Z(\omega)\delta I_{\mathrm{out}}$$

where $\delta I_{\mathrm{in}} = \delta I_g$, $\delta I_{\mathrm{out}} = -\delta I_D$ according to the usual convention. Solving these equations gives

$$\begin{pmatrix}\delta I_{\mathrm{in}}\\ \delta I_{\mathrm{out}}\end{pmatrix} = \begin{pmatrix}Y_{11} & Y_{12}\\ Y_{21} & Y_{22}\end{pmatrix}\begin{pmatrix}\delta V_G\\ \delta V_D\end{pmatrix}$$

where

$$Y_{11} = i\omega C_{gs} + \frac{r_{ds}G(\omega)}{r_{ds}+Z(\omega)}g_m$$

$$Y_{12} = \frac{G(\omega)}{r_{ds}+Z(\omega)}$$

$$Y_{21} = \frac{r_{ds}}{r_{ds}+Z(\omega)}g_m$$

$$Y_{22} = \frac{1}{r_{ds}+Z(\omega)}$$

and r_{ds}, g_m, and C_{gs} are all quantities given by Pucel *et al.* Note that the presence of $G(\omega)$ makes the transistor intrinsically *bilateral* at high frequencies, even when parasitic capacitances are neglected. Note also that $Z(\omega)$, $G(\omega)\to 0$ as $\omega\to 0$, so that we recover the usual quasi-dc Y matrix of the intrinsic FET.

By using a rather elaborate mathematical technique (the Watson–Sommerfeld transformation [10]; see the Appendix), we can rewrite Z and G in the following form. Let

$$\sigma_n = \left(n+\frac{1}{2}\right)\pi$$

$$\zeta = \frac{\omega}{v_s}L_2$$

$$\alpha = L_2/a$$

$$p = b_0/a.$$

Then

$$Z = \frac{V_p}{I_s}\hat{g}(\zeta)$$

where V_p is the pinch-off voltage, I_s the saturation current as defined by Pucel *et al.*, and

$$\hat{g}(\zeta) = -4\alpha\zeta\sum_{n=0}^{\infty}\frac{\sinh[(1-p)\sigma_n/\alpha]}{\sigma_n^2\cosh(\sigma_n/\alpha)}\cdot\frac{j\sigma_n e^{-j\zeta}-(-1)^n\zeta}{\zeta^2-\sigma_n^2}$$

and

$$G(\omega) = 1 - j\zeta - e^{-j\zeta} + 2j\zeta^2\sum_{n=0}^{\infty}\frac{\cosh(p\sigma_n/\alpha)}{\sigma_n^2\cosh(\sigma_n/\alpha)}\cdot\frac{j\sigma_n e^{-j\zeta}-(-1)^n\zeta}{\zeta^2-\sigma_n^2}.$$

Each term of the infinite series has the factor

$$\frac{j\sigma_n e^{-j\zeta}-(-1)^n\zeta}{\zeta^2-\sigma_n^2}$$

which looks as if it diverges for $\zeta=\pm\sigma_n$. In fact, the numerator also vanishes, so that this factor actually is finite.

IV. Comparison of Modeling and Experimental Results

As we mentioned earlier, the standard equivalent circuit model for the MESFET at high frequencies shown in Fig. 2(a) has, in addition to the usual quasi-dc capacitances C_{gd}, C_{gs}, and C_{ds}, two other elements—C_{dip} and R_i. This is because we must account for the experimental fact that a measurement of the admittance Y_{12}, which should be purely imaginary (it relates the feedback gate current to the drain voltage, which can only be mediated by C_{gd} for low frequencies) [11], reveals that $\mathrm{Re}\,Y_{12}$ is in fact positive and varies with ω^2. Using the circuit topology shown in Fig. 4 yields the following low-frequency value for $\mathrm{Re}\,Y_{12}$:

$$\mathrm{Re}\,Y_{12} \cong \omega^2 C_{\mathrm{dip}} R_i C_{gs}^2. \tag{11}$$

In [12], the response of a real 1-μm transistor is analyzed, and small-signal circuit parameters are given. The bias point for the transistor, which corresponds to these parameters, puts the transistor well into saturation, so that its

response is dominated by the saturated portion of the channel; hence, it constitutes an excellent test of our model. The numbers given in [12] that are relevant to our analysis are

$$C_{dip} = 0.12 \text{ pF}$$

$$C_{gs} = 0.62 \text{ pF}$$

$$R_i = 2.6\ \Omega.$$

Inserting these numbers into (11), we find that the coefficient of ω^2 turns out to be 0.0322 $(\text{ps})^2 \cdot \Omega^{-1}$. Let us now examine what our model predicts for this case: using the Grebene and Ghandhi dc model with a saturation velocity of 1.3×10^7 cm/s and a mobility of 4500 $\text{cm}^2/\text{V-s}$, we find that $p = 0.35$ while the length of saturated channel is $L_2 = 0.6\ \mu$m. The low-frequency expansion of $\text{Re}\, Y_{12}$ is to order ω^2

$$\text{Re}\, Y_{12} \cong \frac{1}{4}\left(\frac{L_2}{v_s}\right)^2 (1+4C_0) r_{ds}^{-1} \omega^2 \tag{12}$$

where

$$C_0 = \sum_{n=0}^{\infty} \frac{\cosh p\dfrac{\sigma_n}{\alpha}}{\sigma_n^3 \cosh \dfrac{\sigma_n}{\alpha}}$$

(an additional factor of 1/2 is needed to go to the asymmetric FET case). Working backward from the value $I_{DSS} = 70$ mA is given in [12], we find that $a = 0.2\mu$m; using the value of r_{ds} from this reference gives a value of 0.024 $(\text{ps})^2 \cdot \Omega^{-1}$, in rough agreement with the equivalent circuit value. If we change v_s to 1.1×10^7 cm/s, we get a value of 0.042 $(\text{ps})^2 \cdot \Omega^{-1}$; the experimental value is bracketed between these limits. It is noteworthy that our results depend so sensitively on the values of saturation velocity, length of channel in saturation, and p used; since all of these quantities are rather ill defined in a real MESFET, the model must be used with care. As we see it, the correct procedure to use is the following:

1) Fit the dc data to derive a value of saturation velocity.
2) Fit the low-frequency data to derive a value of r_{ds} (g_m seems to well calculated from the PHS model, but r_{ds} has a notorious 100-kHz "roll-off," which must be avoided).
3) Evaluate our corrections based on this phenomenological data.

Fig. 6 shows $\text{Re}\, Y_{12}$ as a function of frequency when the saturation velocity is chosen so as to match the equivalent circuit coefficient of ω^2. Curve (a) shows the empirical (equivalent-circuit) dependence and curve (b) is the one predicted by our model. The agreement appears to be excellent well beyond the 12-GHz limit of validity of the equivalent-circuit fit. Extrapolating the equivalent-circuit result to higher frequencies shows that our results depart from it at about 60 GHz.

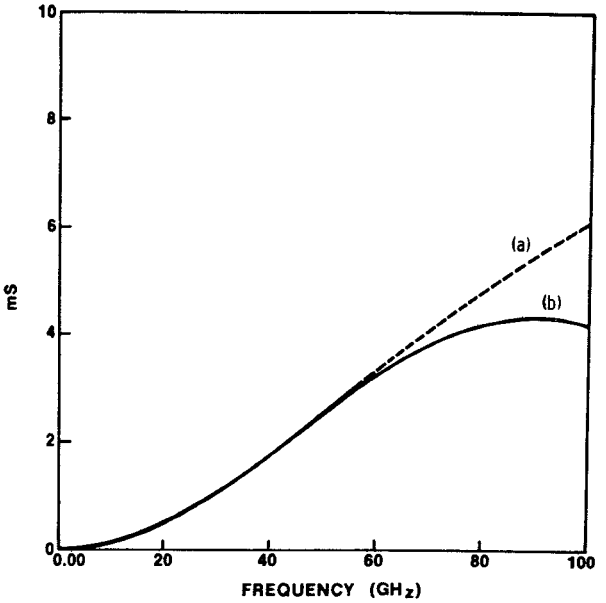

Fig. 6. $\text{Re}\, Y_{12}$ as a function of frequency for (a) the equivalent circuit model with transistor parameters given by Liechti [16], and (b) our model.

V. Discussion

The infinite sums that appear in the definitions of $G(\omega)$ and $Z(\omega)$ are found to resonate at frequencies given by

$$\omega_n = \left(n + \frac{1}{2}\right)\frac{v_s}{L_2} = \left(n + \frac{1}{2}\right)\frac{1}{\tau_s}$$

where τ_s is simply the transit time across the saturated channel (note that these resonances occur at very high frequencies). It is worth noting that if we do not perform the Watson–Sommerfeld transformation, the resonances remain "hidden" in the series (i.e., A_n, B_n, C_n, and D_n show no particular resonant behavior by themselves). Of course, it is not surprising that some resonant behavior should occur in this system. However, our expression for the Y matrix points up a rather significant feature of the analysis: compared to r_{ds}, the modulus of the impedance $Z(\omega)$ actually is quite small, so there is effectively *no transit-time factor* $e^{-j\omega\tau}$ in the transconductance. The reason this factor is absent can be traced to the fact that all high-frequency corrections to the terminal variables are proportional to the drain current $\tilde{\delta} I_D$, whereas only a correction proportional to $\tilde{\delta} V_g$ can affect the transconductance. However, our boundary condition under the gate $[\hat{V}_{\text{HF}}(x, a) = 0]$ automatically eliminates any possibility of space-dependent (i.e., transit time) behavior due to gate-voltage fluctuations. Note that this also is in agreement with experiments: the time τ, which is found empirically from fitting data, is always much smaller than the transit time. Therefore, we suggest that what experimenters are actually seeing is the small complex part of $Z(\omega)$, which gives g_m a small imaginary part, and not some fictitious "phase delay" down the channel. Since $Z(\omega)$ is related to change storage, it is plausible that its effect on the circuit will mimic precisely the type of transit-time delay which the phase factor $e^{-j\omega t}$ is supposed to model; indeed, its

complex value is reminiscent of the "transit angle" which appears in IMPATT theory.

APPENDIX
EVALUATION OF $\hat{g}(\zeta)$ AND $G(\zeta)$

The voltage drop down the channel can be written in the following form:

$$\Delta V = 2Qa \sum_{n=0}^{\infty} [A(\sigma_n) + A(-\sigma_n)] \cos p\sigma_n$$

where

$$A(\sigma) = \frac{-1}{\sigma^2}\left[\frac{\beta(\beta + j\sigma e^{(\sigma - j\beta)\alpha})}{2(\beta^2+\sigma^2)\cosh\alpha\sigma} + \frac{1}{2}\cdot\frac{-j\alpha e^{-j\alpha\beta}}{\beta - j\alpha} - \frac{1}{2}\right]$$

and

$$\sigma_n = \left(n + \frac{1}{2}\right)\pi$$

$$\alpha = L_2/a$$

$$\beta = k_s a$$

$$p = b_0/a.$$

Now, it can be shown that the quantity $A(\sigma)$ has the following properties for complex σ: (a) it is analytic at $\sigma = 0$ and $\sigma = \pm j\beta$, and (b) it has poles at

$$\cosh\alpha\sigma = 0 \rightarrow \sigma = \frac{j}{\alpha}\sigma_n.$$

Applying the Watson–Sommerfeld method, we can write the terms of the sum in the form

$$-2j \sum_{n=-\infty}^{\infty} \oint_{C_n} \frac{dz}{2\pi j} \frac{e^{jpz}}{1+e^{2jz}} A(z)$$

where the contours C_n are shown in Fig. 7(a). Let us deform all these contours into the single contour shown in Fig. 7(b) with $C_{x\pm}, C_{y\pm}$ going off to infinity. It can be shown that the integral vanishes on these contours; after a lengthy computation we obtain

$$\Delta V = +\delta I_D \cdot \frac{V_p}{I_s}\hat{g}(\zeta)$$

where

$$\zeta = \alpha\beta = \omega L_2/v_s$$

and

$$g(\zeta) = -4\alpha\zeta \sum_{n=0}^{\infty} \frac{\sinh[(1-p)\sigma_n/\alpha]}{\sigma_n^2\cosh(\sigma_n/\alpha)} \cdot \frac{j\sigma_n e^{-j\zeta} - (-1)^n\zeta}{\zeta^2 - \sigma_n^2}$$

as stated in the text.

As for the gate charge, using the expressions for A_n, B_n, C_n, and D_n given in the text, we can write δQ_{HF} in the form

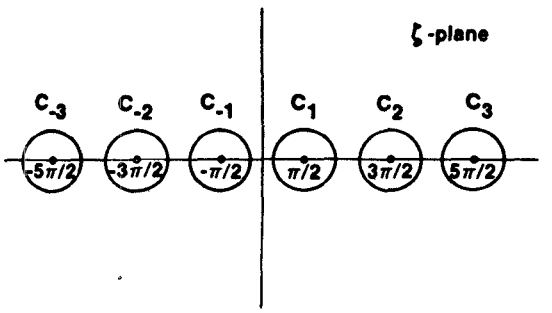

(a)

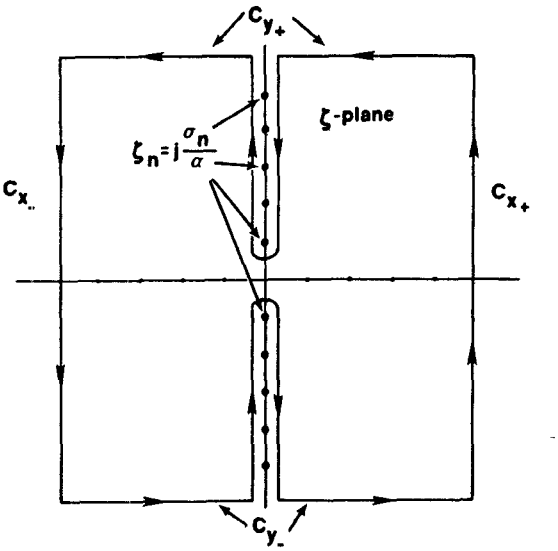

(b)

Fig. 7. Watson–Sommerfeld contours. (a) Contour for the original infinite series (a separate C_n for each series term). (b) A new contour for the entire sum.

$$\delta Q_{HF} = 2\epsilon Qaz \sum_{n=0}^{\infty} (-1)^n \frac{\cos p\sigma_n}{\sigma_n^2}$$

$$\times\left\{\frac{(\beta^2 e^{-j\alpha\sigma_n} + j\beta\sigma_n e^{-j\alpha\beta})(e^{\alpha\sigma_n} - 1)}{(\beta^2+\sigma_n^2)\cosh\alpha\sigma_n}\right.$$

$$-\frac{[\beta^2 e^{-\alpha(-\sigma_n)} + j\beta(-\sigma_n)e^{-j\alpha\beta}][e^{\alpha(-\sigma_n)} - 1]}{(\beta^2+\sigma_n^2)\cosh\alpha\sigma_n}$$

$$\left.-2\alpha\sigma_n - \frac{2\sigma_n^3}{\sigma_n^2+\beta^2}\cdot\frac{e^{-j\alpha\beta}-1}{j\beta}\right\}.$$

Let us rewrite the last two terms, using

$$\alpha\sigma_n + \frac{\sigma_n^3}{\sigma_n^2+\beta^2}\cdot\frac{e^{-j\alpha\beta}-1}{j\beta}$$

$$= \sigma_n\frac{e^{-j\alpha\beta}-1+j\alpha\beta}{j\beta} + j\beta(e^{-j\alpha\beta}-1)\frac{\sigma_n}{\sigma_n^2+\beta^2}$$

and separate them out from ΔQ_{HF}, defining

$$\delta Q_0 = 2\epsilon Qaz \sum_{n=0}^{\infty} (-1)^n \frac{\cos p\sigma_n}{\sigma_n} \cdot \frac{e^{-j\alpha\beta} - 1 + j\alpha\beta}{j\beta}(-2)$$

$$= 2\epsilon Qaz \frac{(-2)}{j\beta}(e^{-j\alpha\beta} - 1 + j\alpha\beta) \sum_{n=0}^{\infty} (-1)^n \frac{\cos p\sigma_n}{\sigma_n}.$$

The sum gives $1/2$, so

$$\delta Q_0 = 2\epsilon Qaz \frac{-1}{j\beta}(e^{-j\alpha\beta} - 1 + j\alpha\beta).$$

Then

$$\delta Q_{HF} = \delta Q_0 + \delta Q_1$$

with

$$\delta Q_1 = 2\epsilon Qaz \sum_{n=0}^{\infty} (-j) \frac{\cos p\sigma_n}{\sigma_n^2}$$

$$\times \left\{ e^{j\sigma_n} \frac{(\beta^2 e^{-\alpha\sigma_n} + j\beta\sigma_n e^{-j\alpha\beta})(e^{\alpha\sigma_n} - 1)}{(\beta^2 + \sigma_n^2)\cosh\alpha\sigma_n} \right.$$

$$+ e^{-j\sigma_n} \frac{[\beta^2 e^{-\alpha(-\sigma_n)} + j\beta(-\sigma_n)e^{-j\alpha\beta}][e^{\alpha(-\sigma_n)} - 1]}{(\beta^2 + \sigma_n^2)\cosh\alpha\sigma_n}$$

$$- j(-1)^n \cdot \beta(e^{-j\alpha\beta} - 1) \frac{2j\sigma_n}{\beta^2 + \sigma_n^2}$$

$$= -2j\epsilon Qaz \sum_{n=0}^{\infty} \cos p\sigma_n$$

$$\left. \times [A'(\sigma_n) + A'(-\sigma_n)] \frac{1}{\sigma_n^2} \right\}$$

where

$$A'(\sigma_n) = e^{j\sigma_n} \frac{(\beta^2 e^{-\alpha\sigma_n} + j\beta\sigma_n e^{-j\alpha\beta})(e^{\alpha\sigma_n} - 1)}{(\beta^2 + \sigma_n^2)\cosh\alpha\sigma_n}$$

$$- \beta(e^{-j\alpha\beta} - 1) \frac{e^{+j\sigma_n}}{\beta - j\sigma_n}$$

is in fact analytic at $\sigma_n = \beta$. Again, a lengthy Watson–Sommerfeld calculation gives

$$\delta Q_1 = 2\epsilon Qaz\alpha\beta \sum_{n=-\infty}^{\infty} \frac{1}{\sigma_n^2} \cdot \frac{\cosh(p\sigma_n/\alpha)}{\cosh(\sigma_n/\alpha)}$$

$$\cdot \frac{[(-1)^n\beta - j(\sigma_n/\alpha)e^{-j\alpha\beta}][j - (-1)^n]}{\beta^2 - \sigma_n^2/\alpha^2}$$

so that the total ac gate charge is

$$\delta Q_{HF} = \frac{a}{v_s} \left\{ -\frac{e^{-j\alpha\beta} - 1 + j\alpha\beta}{j\beta} + \alpha\beta \sum_{n=-\infty}^{\infty} \frac{\cosh(p\sigma_n/\alpha)}{\sigma_n^2 \cosh(\sigma_n/\alpha)} \right.$$

$$\left. \cdot \frac{[(-1)^n\beta - j(\sigma_n/\alpha)e^{-j\alpha\beta}][j - (-1)^n]}{\beta^2 - \sigma_n^2/\alpha^2} \right\} \delta\tilde{I}_D.$$

We now multiply this by $j\omega$ to get the ac gate current:

$$\delta\tilde{I}_g = G\delta\tilde{I}_D$$

where

$$G = 1 - j\alpha\beta - e^{-j\alpha\beta} + j\beta^2\alpha(-2) \sum_{n=0}^{\infty} \frac{\cosh(p\sigma_n/\alpha)}{\sigma_n^2 \cosh(\sigma_n/\alpha)}$$

$$\cdot \frac{[(-1)^n\beta - j(\sigma_n/\alpha)e^{-j\alpha\beta}]}{\beta^2 - \sigma_n^2/\alpha^2}$$

is the dimensionless source strength given in the text.

References

[1] S. M. Sze, *Physics of Semiconductor Devices*. New York: Wiley, 1981, ch. 6.

[2] R. A. Pucel, "Design considerations for monolithic microwave circuits," *IEEE Trans. Microwave Theory Tech.*, vol. MTT-29, pp. 513–534, June 1981.

[3] A. B. Grebene and S. K. Ghandhi, "General theory of pinched operation of the junction gate FET," *Solid-State Electron.*, vol. 12, pp. 573–589.

[4] R. A. Pucel, H. A. Haus, and H. Statz, "Signal and noise properties of gallium arsenide microwave field-effect transistors," in *Advances in Electronics and Electron Physics*, L. Martin, Ed., vol. 38. New York: Academic Press, pp. 175–265, 1975.

[5] G. D. Vendelin and M. Omori, "Circuit models for the GaAs MESFET valid to 12 GHz," *Electron. Lett.*, vol. 11, no. 3, pp. 60–61, Feb. 1975.

[6] W. Shockley, "A unipolar field effect transistor," *Proc. IRE*, vol. 40, pp. 1365–1376, Nov. 1952.

[7] W. Fischer, "Equivalent circuit and gain of MOSFETs," *Solid-State Electron.*, vol. 9, pp. 71–81, 1966; R. H. Dawson, "Equivalent circuit of the Schottky-barrier field-effect transistor at microwave frequencies," *IEEE Trans. Microwave Theory Tech.*, vol. MTT-23, pp. 499–501, June 1975.

[8] S. M. Sze, *Physics of Semiconductor Devices*. New York: Wiley, 1981, ch. 10.

[9] J. D. Jackson, *Classical Electrodynamics*. New York: Wiley, 1962, sec. 1.9.

[10] R. P. Leavitt and C. A. Morrison, "Techniques for evaluating sums by means of complex integration," *Am. J. Phy.*, vol. 50, pp. 1112–1117, Dec. 1982.

[11] G. D. Vendelin, "Feedback effects in the GaAs MESFET model," *IEEE Trans. Microwave Theory Tech.*, vol. MTT-24, pp. 383–385, June 1976.

[12] C. A. Liechti, "Microwave field-effect transistors—1976," *IEEE Trans. Microwave Theory Tech.*, vol. MTT-24, pp. 279–300, June 1976.

✠

Frank J. Crowne did graduate work on theoretical modeling of electron-hole droplets in Si and Ge at Brown University, from which he obtained the Ph.D. in 1975.

He joined the Martin Marietta Laboratories in November 1982, and is currently providing theoretical support for the MMIC program in the area of device modeling. He also does microscopic band-structure modeling of III–V compounds, as well as modeling of superlattices, quantum wells, and other microstructure systems. Prior to joining Martin Marietta, Dr. Crowne was employed for eight years in the Applied Physics Branch, at Harry Diamond Laboratories, where he worked on the physics of semiconductors, lasers and nonlinear optics.

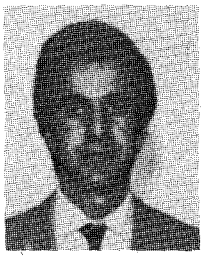

Abdollah Eskandarian obtained the Ph.D. in June 1985.

Since joining Martin Marietta Laboratories in July 1985, he has been working on the modeling and testing of active devices and passive components for microwave and millimeter-wave integrated circuits. Prior to joining Martin Marietta Laboratories, Dr. Eskandarian was a graduate student at Rensselaer Polytechnic Institute, where he worked on solar cells, anodization of GaAs, GaAs MIS capacitors, and low-frequency noise in GaAs Schottky diodes and MESFET's.

✠

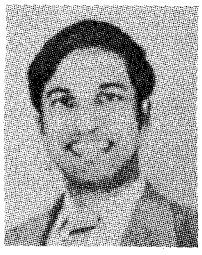

H. Brian Sequeira obtained the B.S. degree from the University of Bombay, India, in 1970, the M.S. degree in physics from IIT, Bombay, in 1972, and the M. Tech. degree in engineering from IISc, Bangalore, in 1974.

He joined Martin Marietta Laboratories in June 1982 and is currently investigating modeling and testing of *Ka*-band devices and circuits. He is also developing active impedance-matched devices for wide-band applications, and Microslab,™ a novel waveguide medium which he invented in 1983. Prior to joining Martin Marietta, Dr. Sequeira earned the Ph.D. degree at the University of Deleware, where he fabricated double-heterostructure GaAs–AlGaAs lasers integrated monolithically with a thermoelectric Peltier cooler. He previously designed and tested radar front-ends for a command-link system.

✠

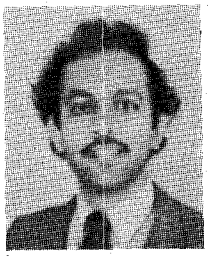

Rajendra Jakhete obtained the B.S. degree in chemical engineering from the University of Bombay, India, in 1978, and the M.S. degree in chemical engineering from Illinois Institute of Technology in 1980. He is currently pursuing the M.S. degree in computer science at Johns Hopkins University.

He joined Martin Marietta Laboratories in November 1980. His current activities in support of GaAs technology include passive comoponent modeling, simulation, computer-aided circuit design, and data base management. Previously, Mr. Jakhete worked in the areas of automatic process control, thermal modeling for electronic devices and packages, process development, simulation, pollution control, and biotechnology.